TRAJECTORY TRACKING $\mathcal{H}_2$ CONTROLLER FOR AUTONOMOUS HELICOPTERS: AN APPLICATION TO INDUSTRIAL CHIMNEY INSPECTION

B. Guerreiro * **C. Silvestre** * **R. Cunha** *
D. Antunes *

* *Instituto Superior Técnico, Institute for Systems and Robotics Av. Rovisco Pais, 1, 1049-001 Lisboa, Portugal*
{cjs,bguerreiro,rita,dantunes}@isr.ist.utl.pt

Abstract: This paper addresses the problem of industrial chimney inspection using autonomous helicopters. The importance of using these platforms is evidenced by the maintenance cost and risk reduction stemming from the replacement of the standard procedures and the improved detection of structural defects. The approach presented relies on the definition of a trajectory-dependent error space to express the dynamic model of the vehicle, and adopts a Linear Parameter Varying (LPV) representation with piecewise affine dependence on the parameters to model the error dynamics over a set of predefined operating regions. The synthesis problem is stated as a continuous-time $\mathcal{H}_2$ control problem, solved using Linear Matrix Inequalities (LMIs) and implemented within the scope of gain-scheduling control theory. The effectiveness of the proposed controller is assessed in simulation using the full nonlinear model of a small-scale helicopter.

Keywords: Autonomous vehicles, helicopter control, disturbance rejection;

1. INTRODUCTION

In this paper the problem of critical infrastructure inspection using autonomous helicopters is considered. Within the scope of Unmanned Aerial Vehicles, autonomous helicopters have been steadily growing a major topic of research. They have the potential to perform high precision tasks in challenging and uncertain operation scenarios as new sensor technology and increasingly powerful computational systems are available.

As discussed in (CICIND, 2006), industrial chimney inspection can be of crucial importance to the proper operation of power plants or other industrial facilities. Industrial chimneys are subjected to high temperatures, chemical attack as well as the effects of weather exposure, that can lead to severe structural deterioration. Hence, they have to be submitted to regular inspection and maintenance procedures (limited to the accessible areas), in order to remain safe and fit for continued service. Otherwise, the consequences widen up from damage to surrounding buildings and loss of production to injury or even loss of human life. The idea of automatic structure inspection is raising the interest of the maintenance industry, and autonomous helicopters arise as natural platforms for this kind of missions, since they can carry multiple sensors, like multi-spectral camera, sonar,

[1] This work was partially supported by Fundação para a Ciência e a Tecnologia (ISR/IST pluriannual funding) through the POS_Conhecimento Program that includes FEDER funds. The work of B. Guerreiro and D. Antunes was supported by PhD Student Grants from the Portuguese FCT POCTI programme.

radar, etc. In the present scenario, the helicopter is expected to follow complex three-dimensional trajectories, and if necessary hover at exact locations, to monitor particular characteristics and assess maintenance or repair requirements. In this context, the development of trajectory tracking control systems constitutes both a challenge and a fundamental requirement for accomplishing high performance autonomous flight.

The presented solution relies on the definition of a trajectory-dependent error space to express the dynamic model of the vehicle. The error vector, which the trajectory-tracking controller should drive to zero, comprises linear and angular velocities, orientation, and position errors relatively to the reference trajectory.

Linear Matrix Inequalities (LMIs) used together with Linear Parameter Varying models (LPVs) constitute a powerful tool for tackling difficult nonlinear problems. Several examples in the literature attest for its level of success (see (Cunha *et al.*, 2006) and references therein). This paper adopts an LPV representation with piecewise affine dependence on the parameters to accurately model the error dynamics over a predefined set of operating regions. By imposing an affine parameter dependence, a continuous-time $\mathcal{H}_2$ state feedback controller can be derived in order to guarantee $\mathcal{H}_2$ performance over a convex set of parameters using a finite number of LMIs. Based on this result, a controller is synthesized for each of the operating regions and the resulting controller is implemented within the framework of gain-scheduling control theory using the D-methodology (Kaminer *et al.*, 1995).

This paper is organized as follows: Section 2 presents a brief summary of the helicopter dynamic model; Section 3 introduces the trajectory-dependent error space; Section 4 deals with the control synthesis; implementation issues and the simulation results are presented in Section 5 and finally Section 6 summarizes the main ideas of this paper and discusses directions for future work.

2. HELICOPTER DYNAMIC MODEL

This section summarizes the helicopter dynamic model. A comprehensive coverage of helicopter flight dynamics can be found in (Padfield, 1996) and (Cunha, 2002; Cunha *et al.*, 2005), where this model is described in more detail.

Consider the helicopter modeled as a rigid body driven by forces and moments applied to the helicopter's center of mass that include the contribution of the main rotor, tail rotor, fuselage, horizontal tail plane, vertical tail fin, and gravity. Define $\{I\}$ as the inertial frame and $\{B\}$ as the Body-fixed frame, with origin at the center of mass. Let $(\mathbf{p}, \mathcal{R}) \in SE(3) \triangleq \mathbb{R}^3 \times SO(3)$ denote the configuration of $\{B\}$ relative to $\{I\}$ where $\mathcal{R}$ can be parameterized by the Z-Y-X Euler angles $\boldsymbol{\lambda} = \left[\, \phi_B \;\; \theta_B \;\; \psi_B \,\right]^T$, $\theta_B \in]-\frac{\pi}{2}, \frac{\pi}{2}[$, $\phi_B, \psi_B \in \mathbb{R}$. In addition, let the linear and angular velocities be given by $\mathbf{v}$ and $\boldsymbol{\omega}$, respectively.

Hence, the helicopter state equations, combining kinematics and dynamics, can be written as

$$\begin{cases} \dot{\mathbf{v}} = -\boldsymbol{\omega} \times \mathbf{v} + \dfrac{1}{m} \left[\mathbf{f}\left(\mathbf{v}, \boldsymbol{\omega}, \mathbf{u}, \mathbf{v}_w\right) + \mathbf{f}_g\left(\phi, \theta\right) \right] \\ \dot{\boldsymbol{\omega}} = -I^{-1}\left(\boldsymbol{\omega} \times I\,\boldsymbol{\omega}\right) + I^{-1}\,\mathbf{n}\left(\mathbf{v}, \boldsymbol{\omega}, \mathbf{u}, \mathbf{v}_w\right) \\ \dot{\mathbf{p}} = \mathcal{R}\left(\boldsymbol{\lambda}\right)\mathbf{v} \\ \dot{\boldsymbol{\lambda}} = \mathcal{Q}\left(\phi, \theta\right)\boldsymbol{\omega} \end{cases}, \quad (1)$$

where m is the vehicle mass, I is the tensor of inertia about the frame $\{B\}$, $\mathbf{u}$ is the input vector, $\mathbf{v}_w$ is the wind velocity vector expressed in $\{B\}$, $\mathbf{f}_g$ represents the gravitational force vector and $\mathbf{f}$ and $\mathbf{n}$ denote the remaining external forces and moments applied to the vehicle. Matrix $\mathcal{Q}$ relates the vehicle angular velocity with the time derivative of the Euler angles. The input vector $\mathbf{u} = \left[\, \theta_{c_0} \;\; \delta_{c_{1c}} \;\; \delta_{c_{1s}} \;\; \theta_{c_{0t}} \,\right]$ comprises the main rotor collective, longitudinal cyclic and lateral cyclic blade pitch angle commands and the tail rotor collective blade pitch angle command, respectively. Note that depending on the complexity of model considered for the blade flap and pitch motions, additional state variables may be required.

The disturbance input $\mathbf{v}_w$ can be modeled as a random process with a predefined power spectral density (PSD) such as the von Karman turbulence model, or using the statistical discrete gust approach (SDG), essentially employed to cater for more structured disturbances. For in depth coverage of this topic the reader is referred to (Padfield, 1996), and references therein.

The force and moment vectors, $\mathbf{f}$ and $\mathbf{n}$, can be further decomposed as $\mathbf{f} = \mathbf{f}_{mr} + \mathbf{f}_{tr} + \mathbf{f}_{fus} + \mathbf{f}_{tp} + \mathbf{f}_{fn}$ and $\mathbf{n} = \mathbf{n}_{mr} + \mathbf{n}_{tr} + \mathbf{n}_{fus} + \mathbf{n}_{tp} + \mathbf{n}_{fn}$, where the subscripts mr, tr, fus, tp and fn stand for main rotor, tail rotor, fuselage, horizontal tail plane and vertical tail fin, respectively.

3. GENERALIZED ERROR DYNAMICS

This section introduces the concepts of trimming trajectories for the helicopter model, presents a generalized error space to describe the helicopter's motion about trimming trajectories, and computes explicitly the helicopter dynamics in the new error space.

Consider the helicopter equations of motion presented in (1), and let $\mathbf{v}_c$, $\boldsymbol{\omega}_c$, $\mathbf{p}_c$, $\boldsymbol{\lambda}_c$, and $\mathbf{u}_c$ denote the trimming values of the state and input vectors. At trimming, these vectors satisfy $\dot{\mathbf{v}}_c = \mathbf{0}$, and $\dot{\boldsymbol{\omega}}_c = \mathbf{0}$ implying that $\dot{\mathbf{u}}_c = \mathbf{0}$, $\dot{\phi}_c = 0$, and $\dot{\theta}_c = 0$.

Given the dependence of the gravitational terms on the roll and pitch angles, only the yaw angle can change without violating the equilibrium condition. However, ψ_c satisfies

$$\begin{bmatrix} 0 \\ 0 \\ \dot{\psi}_c \end{bmatrix} = Q\left(\boldsymbol{\lambda}_c\right)\boldsymbol{\omega}_c, \tag{2}$$

and thus the yaw rate, $\dot{\psi}_c$, is constant. As shown in (Silvestre, 2000), trimming trajectories correspond to helices that can be described by

$$\dot{\boldsymbol{\lambda}}_c = \begin{bmatrix} 0 \\ 0 \\ \dot{\psi}_c \end{bmatrix}, \dot{\mathbf{p}}_c = \begin{bmatrix} V_c\cos(\gamma_c)\cos(\dot{\psi}_c t + \psi_0) \\ V_c\cos(\gamma_c)\sin(\dot{\psi}_c t + \psi_0) \\ -V_c\sin(\gamma_c) \end{bmatrix}, \tag{3}$$

where $V_c = \|\mathbf{v}_c\|$ is the linear body speed, γ_c the flight-path angle, and ψ_0 the helix initial condition. The helix can thus be described by the following parametrization

$$\boldsymbol{\xi} = \begin{bmatrix} V_c & \gamma_c & \dot{\psi}_c & \psi_0 \end{bmatrix}^T. \tag{4}$$

Therefore, $\boldsymbol{\xi}$ fully parameterizes the set achievable helicopter trimming trajectories $\mathcal{E}$ which corresponds to straight lines and z aligned helices described by the vehicle with arbitrary linear speed and yaw angle.

The generalized error vector defined between the vehicle state and the commanded trajectory $\mathcal{E}(\boldsymbol{\xi})$ can be defined using the nonlinear transformation

$$\mathbf{x}_e = \begin{bmatrix} \mathbf{v}_e \\ \boldsymbol{\omega}_e \\ \mathbf{p}_e \\ \boldsymbol{\lambda}_e \end{bmatrix} = \begin{bmatrix} \mathbf{v} - \mathbf{v}_c \\ \boldsymbol{\omega} - \boldsymbol{\omega}_c \\ \mathcal{R}^{-1}\left(\mathbf{p} - \mathbf{p}_c\right) \\ \mathcal{Q}^{-1}\left(\boldsymbol{\lambda} - \boldsymbol{\lambda}_c\right) \end{bmatrix}. \tag{5}$$

In addition, let $\mathbf{u}_e = \mathbf{u} - \mathbf{u}_c$ and $\mathbf{v}_{w_e} = \mathbf{v}_w$, and assume that there is no disturbance at trimming, i.e. $\mathbf{v}_w = 0$. It can be shown that in the new error coordinate system the linearization of the rigid body dynamics given by (1) along any arbitrary trajectory in $\mathcal{E}$ is time invariant, see (Silvestre, 2000) for further details. The nonlinear error dynamics can then be expressed as

$$\begin{cases} \dot{\mathbf{v}}_e = \dot{\mathbf{v}} \\ \dot{\boldsymbol{\omega}}_e = \dot{\boldsymbol{\omega}} \\ \dot{\mathbf{p}}_e = \mathbf{v} - \mathcal{R}_e^{-1}\,\mathbf{v}_c - S(\boldsymbol{\omega})\,\mathbf{p}_e \\ \dot{\boldsymbol{\lambda}}_e = \boldsymbol{\omega} - \mathcal{Q}^{-1}\,\mathcal{Q}_c\,\boldsymbol{\omega}_c - \dfrac{d}{dt}\mathcal{Q}^{-1}\,\mathcal{Q}\,\boldsymbol{\lambda}_e, \end{cases} \tag{6}$$

since $\dot{\mathbf{v}}_c = 0$ and $\dot{\boldsymbol{\omega}}_c = 0$ for any trimming trajectory, and defining $\mathcal{R}_e^{-1} = \mathcal{R}^{-1}\mathcal{R}_c$, $\mathcal{Q}_e = \mathcal{Q}\left(\boldsymbol{\lambda}_e\right)$ and $S(\boldsymbol{\omega})$ as the skew symmetric matrix given by $S(\boldsymbol{\omega}) = [\boldsymbol{\omega}\times]$.

The linearization of (6) about the zero, or equivalently, the linearization of (1) about the trimming trajectory $\mathcal{E}_c$ can be expressed in the generalized error space as

$$\begin{cases} \delta\dot{\mathbf{v}}_e = A_v^v\,\delta\mathbf{v}_e + A_v^\omega\,\delta\boldsymbol{\omega}_e + A_v^\lambda\,\delta\boldsymbol{\lambda}_e + B_v\,\delta\mathbf{u}_e + B_{w_v}\,\delta\mathbf{v}_w \\ \delta\dot{\boldsymbol{\omega}}_e = A_\omega^v\,\delta\mathbf{v}_e + A_\omega^\omega\,\delta\boldsymbol{\omega}_e + A_\omega^\lambda\,\delta\boldsymbol{\lambda}_e + B_\omega\,\delta\mathbf{u}_e + B_{w_\omega}\,\delta\mathbf{v}_w \\ \delta\dot{\mathbf{p}}_e = \delta\mathbf{v}_e - S(\boldsymbol{\omega}_c)\,\delta\mathbf{p}_e - S(\mathbf{v}_c)\,\delta\boldsymbol{\lambda}_e \\ \delta\dot{\boldsymbol{\lambda}}_e = \delta\boldsymbol{\omega}_e - S(\boldsymbol{\omega}_c)\,\delta\boldsymbol{\lambda}_e \end{cases} \tag{7}$$

where $A_x^y = \left.\frac{\partial}{\partial\mathbf{y}}\mathbf{f}_x(.)\right|_c$ are constant matrices for each trimming trajectory, and $\mathbf{f}_x(.)$ represents the functions $\dot{\mathbf{v}} = \mathbf{f}_v\left(\mathbf{v},\boldsymbol{\omega},\boldsymbol{\lambda},\mathbf{u},\mathbf{v}_w\right)$ and $\dot{\boldsymbol{\omega}} = \mathbf{f}_\omega\left(\mathbf{v},\boldsymbol{\omega},\boldsymbol{\lambda},\mathbf{u},\mathbf{v}_w\right)$. Rewriting (7) in a compact form gives

$$\begin{cases} \delta\dot{\mathbf{x}}_e = A_e(\boldsymbol{\xi})\,\delta\mathbf{x}_e + B_{w_e}(\boldsymbol{\xi})\,\delta\mathbf{v}_w + B(\boldsymbol{\xi})\,\delta\mathbf{u}_e \\ \mathbf{z}_e = C_e(\boldsymbol{\xi})\,\delta\mathbf{x}_e + D_e(\boldsymbol{\xi})\,\delta\mathbf{v}_w + E(\boldsymbol{\xi})\,\delta\mathbf{u}_e. \end{cases}$$

From this result it follows that there is a linear time invariant plant (7), associated to each trimming trajectory $\mathcal{E}(\boldsymbol{\xi})$, for which a linear controller can be designed.

4. CONTROLLER SYNTHESIS

In this section an LMI approach is used to tackle the continuous-time state feedback $\mathcal{H}_2$ synthesis problem for polytopic LPV systems. Consider a LPV system of the form

$$\begin{cases} \dot{\mathbf{x}} = A(\boldsymbol{\xi})\mathbf{x} + B_w(\boldsymbol{\xi})\mathbf{w} + B(\boldsymbol{\xi})\mathbf{u} \\ \mathbf{z} = C(\boldsymbol{\xi})\mathbf{x} + D(\boldsymbol{\xi})\mathbf{w} + E(\boldsymbol{\xi})\mathbf{u} \end{cases} \tag{8}$$

where $\mathbf{x}$ is the state, $\mathbf{u}$ is the control input, $\mathbf{z}$ denotes the error signal to be controlled, and $\mathbf{w}$ denotes the exogenous input signal. The system is parameterized by $\boldsymbol{\xi}$, which is a possibly time-varying parameter vector and belongs to the convex set $\Xi = \mathrm{co}(\Xi_0)$ where co(.) denotes the convex hull, Ξ_0 is the set of n_v vertices defined by $\Xi_0 = \{\boldsymbol{\xi} \in \mathbb{R}^{n_p} | \xi_i \in \{\underline{\xi}_i, \overline{\xi}_i\}, i = 1,\ldots,n_p\}$, where $\underline{\xi}_i \leq \overline{\xi}_i$, and the parameter set is defined by $\Xi = \{\boldsymbol{\xi} \in \mathbb{R}^{n_p} | \xi_i \in [\underline{\xi}_i, \overline{\xi}_i], i = 1,\ldots,n_p\}$.

Since the synthesis problem involves testing an infinite number of LMI's, several different structures for the LPV system have been proposed which reduce the problem to that of solving a finite number of LMI's. This paper adopts a polytopic description, which can be used to model a wide spectrum of systems and, as shown in the next section, is an adequate choice for the system at hand.

Definition 4.1. (Polytopic LPV system). The system (8) is said to be a polytopic LPV system if, for all $\boldsymbol{\xi} \in \Xi$, the system matrix $S(\boldsymbol{\xi}) = \begin{bmatrix} A(\boldsymbol{\xi}) & B_w(\boldsymbol{\xi}) & B(\boldsymbol{\xi}) \\ C(\boldsymbol{\xi}) & D(\boldsymbol{\xi}) & E(\boldsymbol{\xi}) \end{bmatrix}$ verifies $S(\boldsymbol{\xi}) \in \mathrm{co}\left(S_1,\ldots,S_r\right)$, where co(.) denotes the convex hull operator and $S_i = \begin{bmatrix} A_i & B_{w_i} & B_i \\ C_i & D_i & E_i \end{bmatrix}$, for all $i = \{1,\ldots,r\}$.

The objective is to find a solution to the continuous-time state feedback $\mathcal{H}_2$ synthesis problem. Con-

sider the static state feedback law given by $\mathbf{u} = K\mathbf{x}$ and let T_{zw} denote the closed loop operator from $\mathbf{w}$ to $\mathbf{z}$. Then, the $\mathcal{H}_2$ synthesis problem can be described as that of finding a control matrix K that stabilizes the closed-loop system and minimizes the $\mathcal{H}_2$ norm $\|T_{zw}\|_2$ of T_{zw}. Note that matrix $D(\boldsymbol{\xi}) = 0$ in order to guarantee that $\|T_{zw}\|_2$ is finite for every internally stabilizing and strictly proper controller. The technique used for controller design relies on results available in (Ghaoui and Niculescu, 1999) and (Scherer and Weiland, 2000), after being rewritten for the case of polytopic LPV systems. In the following, $\mathrm{tr}(L)$ denote the trace of matrix L.

Result 4.1. A static state feedback controller guarantees the α upper-bound for the continuous-time $\mathcal{H}_2$ norm of the closed loop operator $T_{zw}(\boldsymbol{\xi})$ with $\boldsymbol{\xi} \in \Xi$, that is,

$$\|T_{zw}(\boldsymbol{\xi})\|_2 < \alpha, \forall \boldsymbol{\xi} \in \Xi \tag{9}$$

if there are real matrices $X = X^T \succ 0$, $Y \succ 0$ and W such that

$$\begin{bmatrix} A(\boldsymbol{\xi})\,X + X\,A(\boldsymbol{\xi})^T + B(\boldsymbol{\xi})\,W + W^T\,B(\boldsymbol{\xi})^T & B_w(\boldsymbol{\xi}) \\ B_w(\boldsymbol{\xi})^T & -I \end{bmatrix} \prec 0$$

$$\begin{bmatrix} Y & C(\boldsymbol{\xi})\,X + E(\boldsymbol{\xi})\,W \\ X\,C(\boldsymbol{\xi})^T + W^T\,E(\boldsymbol{\xi})^T & X \end{bmatrix} \succ 0$$

$$\mathrm{tr}\,(Y) < \alpha^2\,.$$

for all $\boldsymbol{\xi} \in \Xi_0$. The respective controller gain matrix is given by $K = W\,X^{-1}$.

The optimal solution for the continuous-time $\mathcal{H}_2$ control problem is approximated through the minimization of α subject to the LMIs presented Result 4.1.

5. IMPLEMENTATION AND RESULTS

To perform accurate structure inspection, an autonomous helicopter is required to cover the selected surfaces of the structure comprehensively in order to detect cracks, corrosion, etc. Therefore, in this kind of applications, the required flight envelope is characterized by low speed, high yaw maneuverability, good vertical flight capabilities, and the possibility of describing helices around the structure. Recalling that the parameter vector is given by $\boldsymbol{\xi} = \begin{bmatrix} V_c & \dot{\psi}_c & \gamma_c & \psi_0 \end{bmatrix}$, in the proposed case study the error space is partitioned into 225 convex regions, with $2^4 = 16$ vertices each. For parameters V_c and $\dot{\psi}_c$ only one interval is considered, while parameters γ_c and ψ_0 are partitioned into the 9 and 15 overlapping intervals presented in Table 1.

The state space matrices of the continuous-time systems (8) are approximated by affine functions of $\boldsymbol{\xi}$ using Least Squares Fitting. To evaluate the error introduced by this approximation, the resulting systems were compared with the original ones for each zone, and the average relative error on the matrix entries was always less than 6.49%.

Table 1. Operating regions intervals

Param.	Intervals	Unit
V_c	$[-3, 3]$	$[m/s]$
$\dot{\psi}_c$	$[-0.2, 0.2]$	$[rad/s]$
γ_c	$[-100, -85]$, $[-90, -60]$, $[-65, -35]$, $[-40, -10]$, $[-15, 15]$, $[10, 40]$, $[35, 65]$, $[60, 90]$, $[85, 100]$	$[deg]$
ψ_0	$[-190, -160]$, $[-165, -135]$, $[-140, -110]$, $[-115, -85]$, $[-90, -60]$, $[-65, -35]$, $[-40, -10]$, $[-15, 15]$, $[10, 40]$, $[35, 65]$, $[60, 90]$, $[85, 115]$, $[110, 140]$ $[135, 165]$, $[160, 190]$	$[deg]$

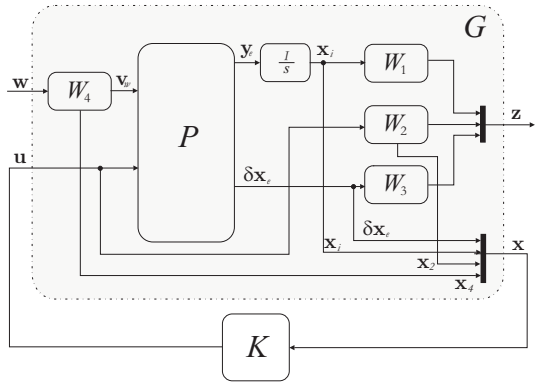

Fig. 1. Synthesis model

5.1 Synthesis Model and Control

The linear state feedback controllers were derived to meet the following design specifications: *i*) Achieve zero steady state error for the error variable $\mathbf{y}_e$ defined below and *ii*) Ensure that the actuators are not driven beyond their natural actuation bandwidth, that is $10\,rad/s$.

Consider the feedback system shown in Fig. 1, where P is the continuous-time linear model of the helicopter error dynamics, and K is a state feedback controller to be designed. The augmented system G shown within the dashed line is the synthesis model (that can serve as an interface between the designer and the $\mathcal{H}_2$ controller synthesis algorithm), which is derived from P by appending the depicted weights, that serve as tuning 'knobs', used to meet the desired performance specifications. The variable $\mathbf{w}$ denotes a vector of gaussian white noise with zero mean and unitary intensity and $\mathbf{v}_w$ is the wind velocity disturbance. The integral of $\mathbf{y}_e = \begin{bmatrix} \mathbf{p}_e^T & \psi_e \end{bmatrix}^T$ is included in the design to guarantee that the closed loop system has zero steady-state error in response to linear position and yaw angle commands.

To meet the design requirements the weighting function W_1 is chosen as $W_1 = 0.1\,I_4$, the dynamic

weight associated with the actuation vector $\mathbf{u}$ is $W_2(s) = \mathrm{diag}\left([W_{2a}(s)\,[1\ 1\ 1], W_{2b}(s)]\right)$ where

$$W_{2a}(s) = \frac{13}{10}\,\frac{s+10}{s+13} \quad \text{and} \quad W_{2b}(s) = \frac{10}{7}\,\frac{s+7}{s+10}\,, \tag{10}$$

the state weight is given by $W_3 = 0.1\,I_{12}$ and the dynamic weight associated with the disturbance generation process is

$$W_4(s) = \begin{bmatrix} W_{4u}(s) & 0 & 0 \\ 0 & W_{4v}(s) & 0 \\ 0 & 0 & W_{4w}(s) \end{bmatrix} \tag{11}$$

where $W_{4(.)}(s)$ represent Von Karman disturbance model transfer functions (see (Padfield, 1996) and references therein). In the present case these transfer functions were set to

$$\begin{aligned} W_{4u}(s) &= \frac{\sigma_u\,\sqrt{\frac{2}{\pi}\,\frac{L_u}{V}}\,\left(1 + 0.25\,\frac{L_u}{V}\,s\right)}{1 + 1.357\,\frac{L_u}{V}\,s + 0.199\,(\frac{L_u}{V}\,s)^2} \\ W_{4v}(s) &= \frac{\sigma_v\,\sqrt{\frac{1}{\pi}\,\frac{L_v}{V}}\,\left(1 + 2.748\,\frac{L_v}{V}\,s + 0.34\,(\frac{L_v}{V}\,s)^2\right)}{1 + 2.996\,\frac{L_v}{V}\,s + 1.975\,(\frac{L_v}{V}\,s)^2 + 0.154\,(\frac{L_v}{V}\,s)^3} \\ W_{4w}(s) &= \frac{\sigma_w\,\sqrt{\frac{1}{\pi}\,\frac{L_w}{V}}\,\left(1 + 2.748\,\frac{L_w}{V}\,s + 0.34\,(\frac{L_w}{V}\,s)^2\right)}{1 + 2.996\,\frac{L_w}{V}\,s + 1.975\,(\frac{L_w}{V}\,s)^2 + 0.154\,(\frac{L_w}{V}\,s)^3} \end{aligned}$$

where $\sigma_{(.)}$ denote the turbulence intensity of each component, $L_{(.)}$ are the turbulence scale lengths and V is the aircraft speed norm.

To summarize, the synthesis model G can be written as

$$\begin{cases} \dot{\mathbf{x}} = A(\boldsymbol{\xi})\mathbf{x} + B_w(\boldsymbol{\xi})\mathbf{w} + B(\boldsymbol{\xi})\mathbf{u} \\ \mathbf{z} = C\mathbf{x} + D\mathbf{w} + E\mathbf{u} \end{cases} \tag{12}$$

where $\mathbf{x} = \left[\,\delta\mathbf{x}_e^T\ \mathbf{x}_i^T\ \mathbf{x}_2^T\ \mathbf{x}_4^T\,\right]^T \in \mathbb{R}^{12+4+4+8}$ is the new state vector, $\mathbf{w} \in \mathbb{R}^3$ is the white noise disturbance vector, $\mathbf{u} \in \mathbb{R}^4$ is the actuation vector and the design matrices are given by

$$A(\boldsymbol{\xi}) = \begin{bmatrix} A_e(\boldsymbol{\xi}) & \mathbf{0} & \mathbf{0} & B_{w_e}(\boldsymbol{\xi})\,C_{w_4} \\ C_e & \mathbf{0} & \mathbf{0} & D_e\,C_{w_4} \\ \mathbf{0} & \mathbf{0} & A_{w_2} & \mathbf{0} \\ \mathbf{0} & \mathbf{0} & \mathbf{0} & A_{w_4} \end{bmatrix},$$

$$B_w(\boldsymbol{\xi}) = \begin{bmatrix} B_{w_e}(\boldsymbol{\xi})\,D_{w_4} \\ D_e\,D_{w_4} \\ \mathbf{0} \\ B_{w_4} \end{bmatrix},\ B(\boldsymbol{\xi}) = \begin{bmatrix} B_e(\boldsymbol{\xi}) \\ E_e \\ B_{w_2} \\ \mathbf{0} \end{bmatrix},$$

$$C = \begin{bmatrix} \mathbf{0} & W_1 & \mathbf{0} & \mathbf{0} \\ \mathbf{0} & \mathbf{0} & C_{w_2} & \mathbf{0} \\ W_3 & \mathbf{0} & \mathbf{0} & \mathbf{0} \end{bmatrix},\ E = \begin{bmatrix} \mathbf{0} \\ D_{w_2} \\ \mathbf{0} \end{bmatrix},$$

with $D = \mathbf{0}$ and $[A_{w_i}, B_{w_i}, C_{w_i}, D_{w_i}]$ resulting from the state space representation of $W_i(s)$. Figure 2 depicts the controller implementation scheme based on the D-methodology comprehensively described in (Kaminer *et al.*, 1995). This methodology moves all integrators to the plant input, and adds differentiators where they are needed to preserve the transfer functions and the stability characteristics of the closed loop system. The D-methodology implementation has several important features that are worthwhile emphasizing: i) auto-trimming property - the controller automatically generates adequate trimming values for the actuation signals and for the state variables that are not required to track reference inputs; ii) the implementation of anti-windup schemes is straightforward, due to the placement of the integrators at the plant input.

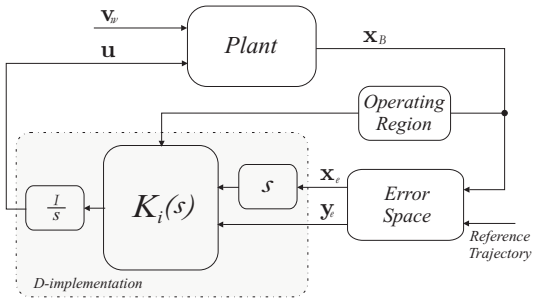

Fig. 2. Implementation setup

5.2 Simulation Results

The simulation results herein presented were obtained using the nonlinear dynamic model SimModHeli, parameterized for the Vario X-Treme model-scale helicopter. The specific application addressed in this paper (industrial chimney inspection) motivated the design of a simulation setup that can effectively be used to evaluate the performance of the overall closed loop system in a real mission scenario. In the present case the inspection of a power plant chimney is considered, see Figure 4. For that purpose the vehicle is required to track the following trajectory: *(i)* a straight line moving sideways ($V_r = 2m/s$, $\psi_c = \pi/2rad$ and $\dot{\psi}_r = \gamma_r = 0$); *(ii)* a helix keeping the camera axis pointing in the direction of the surface under inspection ($V_r = 2m/s$, $\psi_c = \pi/2rad$, $\dot{\psi}_r = 0.24rad/s$ and $\gamma_r = 0.34rad$); and *(iii)* finally a hover at a prespecified point. In addition to the noise generated using the Von Karman disturbance model a discrete wind gust with amplitude $2.5m/s$ and rising time of $1s$ is applied at time $t = 20s$.

The trajectory described by the helicopter and corresponding actuation signals are represented in Figures 3. As shown in the figure, the transitions between the different stages of the trajectory display a smooth behavior. It can be also concluded that the controller is able to reject the wind disturbance induced by the Von Karman model and the overall vehicle trajectory only deviates from the reference when discrete wind gusts are applied.

6. CONCLUSIONS

This paper presented the design and performance evaluation of a 3-D trajectory tracking controller

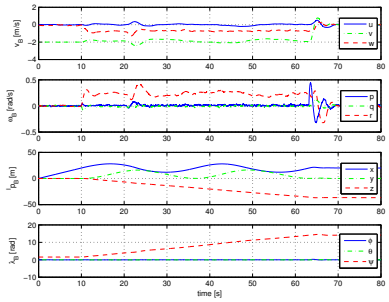

(a) State variables

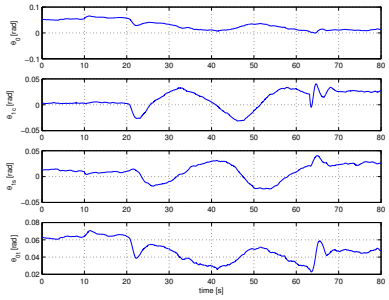

(b) Actuation

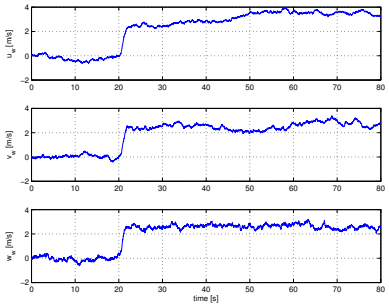

(c) Wind velocity disturbance

Fig. 3. 3-D trajectory following results

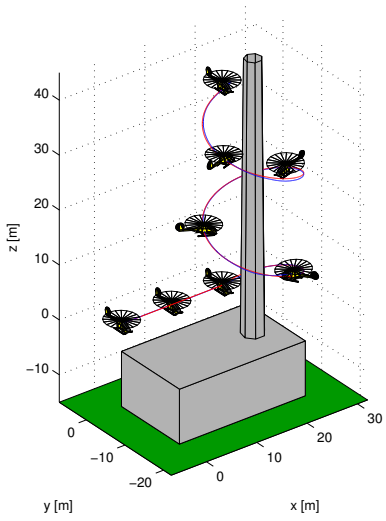

Fig. 4. Inspection scenario

for autonomous helicopters, motivated by the possible use of these vehicles in inspection of industrial infrastructures. Resorting to an $\mathcal{H}_2$ controller design methodology for affine parameter-dependent systems, the technique presented exploited an error vector that naturally describes the particular dynamic characteristics of the helicopter for a suitable flight envelope. For a given set of operating regions, a nonlinear controller was synthesized and implemented under the scope of gain-scheduling control theory, using a piecewise affine parameter-dependent model representation. The effectiveness of the proposed control laws was assessed in the MATLAB/Simulink simulation environment with a nonlinear model of the helicopter in a realistic mission scenario. The quality of the results obtained clearly indicate that the methodology presented is well suited to be used in the proposed application.

REFERENCES

CICIND (2006). *CICIND Chimney Maintenance Guide*. International Committee on Industrial Chimneys (CICIND).

Cunha, Rita (2002). Modeling and control of an autonomous robotic helicopter. Master's thesis. Department of Electrical and Computer Engineering, Instituto Superior Técnico. Lisbon, Portugal.

Cunha, Rita, Bruno Guerreiro and Carlos Silvestre (2005). Vario-xtreme helicopter nonlinear model: Complete and simplified expressions. Technical report. Instituto Superior Técnico, Institute for Systems and Robotics.

Cunha, Rita, Duarte Antunes, Pedro Gomes and Carlos Silvestre (2006). A path-following preview controller for autonomous air vehicles. In: *AIAA Guidance, Navigation and Control Conference*. AIAA. Keystone, CO.

Ghaoui, Laurent and Silviu-Iulian Niculescu (1999). *Advances in Linear Matrix Inequality Methods in Control*. Society for Industrial and Applied Mathematics, SIAM. Philadelphia, PA.

Kaminer, Isaac, António Pascoal, Pramod P. Khargonekar and Edward E. Coleman (1995). A velocity algorithm for the implementation of gain-scheduled controllers. *Automatica* **31**(8), 1185–1191.

Padfield, Gareth D. (1996). *Helicopter Flight Dynamics: The Theory and Application of Flying Qualities and Simulation Modeling*. AIAA Education Series. AIAA. Washington DC.

Scherer, Carsten and Siep Weiland (2000). Lecture notes on linear matrix inequality methods in control. Dutch Institute of Systems and Control.

Silvestre, Carlos (2000). Multi-objective Optimization Theory with Applications to the Integrated Design of Controllers/Plants for Autonomous Vehicles. PhD thesis. Instituto Superior Técnico, Universidade Técnica de Lisboa. Lisbon, Portugal.